HHS Public Access

Author manuscript

J Electrocardiol. Author manuscript; available in PMC 2017 May 01.

Published in final edited form as:

J Electrocardiol. 2016 ; 49(3): 323–336. doi:10.1016/j.jelectrocard.2016.02.014.

Spatial Organization of Acute Myocardial Ischemia

Kedar Aras[*,†,+], **Brett Burton**[*,†,+], **Darrell Swenson**[*,†,+], and **Rob MacLeod**[*,†,+]

[*] Bioengineering Department, University of Utah, Salt Lake City, UT, USA

[†] Cardiovascular Research and Training Institute (CVRTI), Salt Lake City, UT, USA

[+] Scientific Computing Institute (SCI), University of Utah, Salt Lake City, UT, USA

Abstract

Introduction—Myocardial ischemia is a pathological condition initiated by supply and demand imbalance of the blood to the heart. Previous studies suggest that ischemia originates in the subendocardium, i.e., that nontransmural ischemia is limited to the subendocardium. By contrast, we hypothesized that acute myocardial ischemia is not limited to the subendocardium and sought to document its spatial distribution in an animal preparation. The goal of these experiments was to investigate the spatial organization of ischemia and its relationship to the resulting shifts in ST segment potentials during short episodes of acute ischemia.

Methods—We conducted acute ischemia studies in open-chest canines (N=19) and swines (N=10), which entailed creating carefully controlled ischemia using demand, supply or complete occlusion ischemia protocols and recording intramyocardial and epicardial potentials. Elevation of the potentials at 40% of the ST segment between the J-point and the peak of the T-wave (ST40%) provided the metric for local ischemia. The threshold for ischemic ST segment elevations was defined as two standard deviations away from the baseline values.

Results—The relative frequency of occurrence of acute ischemia was higher in the subendocardium (78% for canines and 94% for swines) and the mid-wall (87% for canines and 97% for swines) in comparison with the subepicardium (30% for canines and 22% for swines). In addition, acute ischemia was seen arising throughout the myocardium (distributed pattern) in 87% of the canine and 94% of the swine episodes. Alternately, acute ischemia was seen originating only in the subendocardium (subendocardial pattern) in 13% of the canine episodes and 6% of the swine episodes ($p < 0.05$).

Conclusions—Our findings suggest that the spatial distribution of acute ischemia is a complex phenomenon arising throughout the myocardial wall and is not limited to the subendocardium.

1 Introduction

Despite a century of research and practice, the clinical accuracy of the electrocardiogram (ECG) to detect and localize myocardial ischemia remains less than satisfactory [1].

Myocardial ischemia occurs when the heart does not receive adequate oxygen-rich blood to keep up with its metabolic requirements, and severe ischemia can lead to myocardial infarction and life-threatening arrhythmias. Early and accurate detection is therefore an essential component of managing this condition. In the emergency room (ER), a resting 12-lead ECG is often recorded in patients with symptoms of angina (chest pain). However, such a single resting ECG is normal in up to 50% of patients with chronic, stable angina [2]. Far from static, ischemia is known to be a dynamic condition that reflects a changing imbalance between blood supply and metabolic demand. This dynamic behavior presents diagnostic challenges and encourages continuous monitoring, which is feasible only with a technique like the ECG. Outside the emergency room, it is natural that examination of the ECG under physical stress conditions, or exercise testing (ET), has long been in widespread clinical use. A meta-analysis (24,047 patients with interpretable resting ECG in 147 studies) found exercise ECG without imaging to have a pooled sensitivity of 68% and specificity of 77% for detection of coronary artery disease [2]. Thus, ET is characterized by poor sensitivity and specificity, limiting its diagnostic usefulness. Due to the extremely high incidence of ischemia and the many practical and economical advantages of ECG based testing, any improvements in this technique and the interpretation of the data it gathers will have a profound impact on clinical practice.

The most common clinical ECG marker for myocardial ischemia detection is the ST segment, that portion of the ECG time signal that lies between the QRS complex and the T-wave. Changes in the ST segment can occur within 15–30 seconds after the onset of ischemia [3] and hence represent one of the earliest markers of the condition. The ST segment represents the period when the ventricles are depolarized, *i.e.,* the ventricular action potentials are all in the plateau phase. In a healthy heart, this means that all regions of the ventricles have approximately the same transmembrane potential and that this phase of the normal ECG is isoelectric. However, the ST segment potential can shift above (ST segment elevation) or below (ST segment depression) the baseline during myocardial ischemia, depending on the flow of what are known as “injury currents.” These currents are the result of voltage gradients between normal and ischemic regions, gradients that arise because of differences between the action potentials (AP) of ischemic and normal cells that include localized shortening, diminishing amplitude, and a decrease (more positive value) in resting membrane potential. Furthermore, the change in the resting potential of ischemic cells (due to increased K^+ efflux) causes a TQ segment shift [4], where as the shortening of AP duration due to activation of I_{KATP} channel causes the ST segment shift [5]. A change in the plateau potential to a less positive (more negative) value in the ischemic region, in addition to a shortening of its duration, will also contribute to ST segment changes. Thus, the ST segment elevation on the body surface is a combination of a TQ segment change and ST segment change. The resulting injury currents can produce an ST segment *elevation* in an extracellular or body-surface electrode if they are directed *towards* the recording electrode or ST segment *depression* if they are directed *away* from the electrode.

Classic electrocardiographic theory builds on these biophysically sound concepts with additional assumptions about the spatial distribution of healthy and ischemic tissues; however, these assumptions may be too simplified to explain both experimental and clinical observations. The historical basis for many of these assumptions lies in postmortem

examinations of infarcted hearts [6] under the additional assumption that the location and extent of eventual scar and infarct zones match approximately the ischemic regions that arise acutely following onset of ischemia. Previous studies of acute ischemia were instead based on measured potentials primarily from the epicardial and endocardial surfaces [7]. While surface potentials are a reflection of intramyocardial events, it is only possible to *infer* the underlying bioelectric sources rather than measure them directly. Intramural potentials have also been measured using wick electrodes (10-40 recording sites) [8] but have been limited by low spatial resolution. With the recent development of flexible multiple electrode needles [9] we can now capture extracellular potentials throughout the ventricular wall with high spatial resolution (250 recording sites).

From these early experiments have come several elements that now make up the prevailing putative explanation for clinical observations of ST segments during acute ischemia. Central to this explanation of the spatial dynamics of ischemia is the assumption that at low grades of perfusion deficit, myocardial ischemia is localized to the subendocardium (innermost region of the heart wall) [3]. Justification for this assertion includes the notion that this region has the highest metabolic demand and is the most distal perfusion zone and hence most vulnerable [3]. Moreover, with increased stress, ischemia was thought to progress over time uniformly towards the epicardium (outermost region), eventually becoming transmural (spanning the full thickness of the heart wall). According to this theory, ischemia localized to the subendocardium would generate injury currents flowing away from the epicardial or body-surface electrodes toward the localized subendocardial ischemic region. Thus ST segment depression is thought to indicate subendocardial ischemia. Moreover, transmural ischemia would then produce injury currents flowing towards the recording electrodes located above the affected region of the heart, resulting in ST segment elevations. Many decades of clinical practice and experimental studies have shown that, indeed, superficial leads with ST segment elevation can be linked spatially to the region of ischemia and thus provide a means to localize transmural ischemia from the body surface. However, the same is not true of the ability of ST segment depression to locate nontransmural ischemia [10].

Preliminary results from our group using intramyocardial recordings do not support the assertion that nontransmural ischemia arises only in the subendocardium [11] and have motivated a comprehensive evaluation of the spatial distribution of acute ischemia based on high-resolution measurements under a range of conditions. Our goal in this study was to evaluate the conventional mechanisms for nontransmural ischemia using intramural electrodes to measure three-dimensional potential distributions in the ventricles of animals exposed to acute ischemia. We conducted a series of 29 separate experiments under a range of acute ischemia conditions using two different in situ animal models. To interpret the resulting electrograms, we assumed that localized ischemia causes localized elevations in the extracardiac ST segment potentials. We measured three-dimensional surface and transmural potential distributions under study protocols that altered both the local coronary supply and global metabolic demand.

2 Methods

2.1 Experimental Preparation

The goal of these experiments was to detect the three-dimensional distribution of ischemia-induced shifts in ST segment potentials during the acute phase of short episodes of ischemia created by reduced coronary flow and an increased rate of contraction. We performed experiments on open-chest, intact canines and swines using multipolar intramural needle electrodes and epicardial surface electrodes. Study subjects included 29 animals: 19 purpose bred dogs and 10 adult mini pigs, following the approval from the Institutional Animal Care and Use Committee at University of Utah and conforming to the Guide for the Care and Use of Laboratory Animals (NIH Pub. No 85-23, Revised 1996).

An open-chest preparation following mid-sternal thorocotomy allowed direct access to the heart for recording epicardial potentials from the entire surface of both ventricles and transmural potentials from the anterior aspects of the right and left ventricles. The animal was anesthetized by bolus injection of sodium pentobarbital (30 mg/kg) for canines or isoflurane gas (1–3% inhalant to effect) for pigs, followed by maintenance doses administered as needed. After the thorocotomy, the heart was suspended in a pericardial cradle. Ventilation was with room air mixed with oxygen adjusted to maintain physiological blood gas parameters and pH. A heated and automatically monitored heating table ensured physiological body temperature, and insulation and monitoring maintained stable cavity temperature to minimize any thermally induced repolarization changes. A pacing clip attached to the right atrial appendage provided control of heart rate above the intrinsic rate for each animal.

A suitable left anterior descending (LAD) segment was then dissected and freed from the underlying tissue. For one set of experiments in which we regulated the coronary flow progressively, the LAD was cannulated and perfused by the blood from one of the carotid arteries with flow rates controlled by a digital pump. In a second set of experiments, we circled the LAD using a snare that we closed completely to create ischemic episodes. In a third set of experiments, we circled the LAD using a hydraulic occluder and used it to regulate coronary flow. In this third approach, calibration of the fluid volume injected into the occluder enabled us to perform graded reductions in coronary perfusion. A heat exchanger ensured that the perfused blood was maintained at physiological temperatures. A measurement of coronary flow and intrinsic heart rate at the start of each experiment determined default resting values.

2.2 Experimental Protocols and Data Acquisition

The study protocol was designed to simulate three forms of acute ischemia: 1) a stress test with pacing as a surrogate for exercise, 2) episodes of reduced coronary perfusion to simulate coronary artery disease, and 3) complete occlusion. Mirvis *et al.* have shown that tachycardia increases oxygen demand that is unaffected by mode of tachycardia induction, such as exercise or pacing [12]. Similarly, by combining elevated heart rate and reduced coronary perfusion in different protocols, we were able to simulate both of what are known as “demand” and “supply” types of ischemia. For demand ischemia, characterized by

progressively elevating metabolic demand under stable perfusion conditions, the coronary perfusion was held constant and the pacing rate was increased in a stepwise manner in increments of the pacing interval of 30–50 milliseconds. Supply ischemia, in which demand is stable but blood supply is progressively reduced, was induced by keeping the pacing rate constant and decreasing the perfusion rate in steps of 7–10 ml/min for the cannulated LAD and steps of 25% perfusion deficit when using the hydraulic occluder. For complete occlusion, the coronary perfusion through the selected LAD segment was reduced to zero using a snare. Moreover, the rate was spontaneous (intrinsic) as the heart was not paced for the duration of the ischemic intervention. A total of 100 ischemic episodes were conducted for canine (N=19) studies including 37 demand ischemia, 50 supply ischemia, and 13 complete occlusion protocols. Similarly, a total of 36 ischemic episodes were conducted for swine studies (N=10) including 16 demand ischemia, 18 supply ischemia, and 2 complete occlusion protocols. Each resulting ischemic episode lasted 2–10 minutes depending on the protocol, the intrinsic values of resting heart rate and coronary flow of each animal, and the maximum heart rates tolerated. Each experiment consisted of four to six such episodes separated by recovery periods (at intrinsic heart rates and perfusion) of approximately 25–30 minutes. Electrical recordings (described in detail below) were taken for 3 seconds every 15–20 seconds during the ischemic episode as well as during the recovery period. Fig. 1 contains a schematic of the animal preparation.

Epicardial potentials were recorded from the surfaces of both the ventricles using a 247-electrode flexible sock array, the construction of which is described elsewhere [13]. In addition, up to 25 flexible fiberglass needles [9], each carrying 10 electrodes along its length, spaced at 1.5 mm, were inserted into the ventricles in and around the region presumably perfused by the cannulated or occluded LAD, taking care to avoid injuring the epicardial arteries. The spacing between needles within the epicardial region they covered did not exceed 10 mm. The perfused region was identified before insertion by stopping blood flow through the LAD for 45 seconds and recording the resulting epicardial potentials. Localized ST segment elevations were considered indications of nearby ischemia. The potentials from sock and needle electrodes were recorded using a custom acquisition system permitting simultaneous acquisition of 1024 channels at 1 kHz sampling rate [14]. A band pass filter with cutoff frequencies at 0.03 and 500 Hz avoided both DC potentials and aliasing. A single limb lead was used as a remote reference for all the unipolar signals (AC-coupled) recorded from the sock and needle electrodes. The ST segment elevation recorded with AC-coupled amplifiers represents shift in the TQ segment (TQ depression) and true elevation of the ST segment [15].

2.3 Postexperiment Imaging and Signal Processing

The electrograms recorded during the study were processed in Matmap, a custom MATLAB-based signal processing program developed in our laboratory. The signals were first calibrated and gain adjusted and their baselines corrected. Poor quality signals from sock and needle electrodes, for example due to incomplete contact with the tissue, were discarded. Electrograms recorded from needle electrodes near the tip without positive R-wave deflection were identified as cavity electrodes and also discarded. At the end of the experiment, the locations of preselected sock electrodes and all the plunge needles on the

cardiac surface were digitally recorded using a Microscribe 3D digitizer (Solution Technologies, Inc., Oella, MD). Interactive visualization of the resulting spatio-temporal maps of cardiac potentials was by means of *map3d* [16]. Following each experiment, the heart was excised and scanned with a 7-tesla MRI scanner (Bruker, Inc., Billerica, MA). The resulting image sets were segmented to identify the atria and ventricles using Seg3D [17], and the segmentations became the basis of a volumetric tetrahedral mesh created using SCIRun [18]. The digitized sock and needle electrodes were then registered to this mesh geometry and visualized in SCIRun. Additional visualization and analysis were performed by interpolating potentials on parallel cutting planes regularly spaced through the volume. We differentiated between subendocardial (Endo), midmyocardial (Mid), and subepicardial regions (Epi), as defined by 0–30%, 30–70%, and 70–100% of the distance along those electrodes of each transmural plunge needle that were within the myocardium. Thus, each region roughly spanned one third the thickness of the left ventricular wall. Moreover, ST elevated regions that overlapped into multiple regions (e.g., Endo/Mid) were labeled accordingly.

Elevation of the value of the potentials at 40% of the ST segment between the J-point and the peak of the T-wave (ST40%) provided the metric for local ischemia. The global Root Mean Squared (RMS) signal computed from all the sock and needle electrode electrograms was used to identify J-point and T-peak fiducials. To minimize the effects of signal noise, we first computed the average of 10 potential values around the ST40% time instant. In addition, to minimize the influence of beat to beat fluctuations, we further averaged the ST40% values from three consecutive beats for each electrode site. The results from initial experiments indicated the need to normalize ST segment changes from control recordings taken before each intervention. All ST40% values within the same intervention were evaluated relative to these control values. We also defined a threshold for ischemic ST segment elevations from these normalized ST40% potentials as two standard deviations away from the baseline values. Thus, the derived ST40% potentials were analyzed spatially (up to 500 recording sites) and temporally (approximately every 15 seconds) to track the ST elevated regions during an acute ischemic episode.

2.4 Statistical Analysis

A chi-square test of goodness-of-fit was performed to determine whether the spatial distribution of acute ischemia—subendocardial, and distributed—were equally preferred. The subendocardial group comprised episodes which resulted in ST elevated regions localized in the subendocardial region (“Endo”) and/or spanned the subendocardial region and also extended into the midmyocardial region (“Endo/Mid”). Thus, if all the identified ST elevated regions during the course of an acute ischemic episode originated exclusively in the subendocardium, the episode was categorized into the subendocardial group. Alternately, the distributed group comprised episodes that resulted in ST elevated regions arising throughout the left ventricular wall including subendocardial, midmyocardial and subepicardial regions during the course of an ischemic episode. Thus, if at least one of the identified ST elevated regions during the course of an ischemic episode originated in the mid-wall (“Mid”), subepicardium (“Epi”), or the overlapping region(“Mid/Epi”), the episode was classified as part of the distributed group. Moreover, each defined region was counted only once for

calculating the relative frequency of occurrence, even if there were multiple ST elevated regions in the defined region during the course of an ischemic episode. Statistical significance was set at alpha < 0.05.

3 Results

In the experiments, we found examples of ischemia distributed over most of the ventricular wall. We show here four representative examples of ischemia measured in the subendocardium, the mid-wall, and the subepicardium together with two statistical summaries of relative frequency of occurrence across all 29 experiments.

Fig. 2 highlights data from a canine complete occlusion study in which acute ischemia was distributed in multiple, separate regions across the ventricular wall, all within the same ischemic intervention. Panel A shows the intramural ischemic volume. The onset of ischemia, which occurred 30 seconds into the intervention was characterized by three ST segment elevated regions (in red) exceeding the threshold of two standard deviations from baseline (4 mV). Panel B columns show the location of the ischemic regions in the mid-wall (S1), subepicardium (S2), and the subendocardium (S3) respectively. The epicardial surface did not show any meaningful ST-segment shifts at this stage. However, by the end of the intervention (180 seconds), the ST elevated regions had merged and reached transmural status as also reflected on the epicardial surface with ST segment elevation localizing the underlying ischemia.

Fig. 3 highlights data from a canine supply ischemia study (@ 172 BPM) in which acute ischemia was also distributed in multiple, separate regions across the ventricular wall. The onset of ischemia, which occurred 270 seconds into the intervention (75% perfusion deficit) was characterized by two ST segment elevated regions in the subendocardium (S1), and the mid-wall (S2) respectively. The epicardial surface once again did not show any meaningful ST-segment shifts at this stage. However, the ST elevated regions also reached transmural status and was reflected on the epicardial surface with ST segment elevation localizing the underlying ischemia.

Fig. 4 highlights data from a canine demand ischemia study (50% perfusion deficit) in which acute ischemia was distributed in multiple, separate regions across the ventricular wall. The onset of ischemia, which occurred 320 seconds into the intervention (200 BPM) was characterized by one ST segment elevated region in the subendocardium (S1). The epicardial surface showed a sharp ST-segment depression at this stage that covered an area wider than the underlying ischemic region. By the end of the intervention (480 seconds) there were additional ST elevated regions arising throughout the ventricular wall including the mid-wall region (S2). However, none of the ischemic regions reached transmural status. The corresponding epicardial surface potential difference map showed the sharp ST segment depression spanning a much wider region, relative to the underlying ischemic regions.

Fig. 5 highlights data from a swine supply ischemia (@ 133 BPM) study in which acute ischemia originated in the mid-wall region. The onset of ischemia, which occurred 270 seconds into the intervention (75% perfusion deficit) was characterized by one ST segment

elevated region in the mid-wall (S1) region. The epicardial surface did not show any meaningful ST-segment shifts similar to that seen in canine studies.

Figure 6 contains a summary of ischemia distribution resulting from studies across all 19 canine animals. The histograms of relative frequency of occurrence of acute ischemia in each of the three defined regions (Endo, Mid, Epi) as well as the two overlapping regions are shown. Panel A shows the cumulative spatial distribution of acute ischemia across all ischemic episodes (n=100). Panel B shows the spatial distribution of acute ischemia during demand ischemia episodes (n=37). Panel C shows the spatial distribution of acute ischemia during supply ischemia episodes (n=50). Panel D shows the histograms of relative frequency of occurrence of acute ischemia categorized as conventionally arising in the subendocardium (Subendocardial) or arising across the ventricular wall (Distributed). The relative frequency of occurrence of acute ischemia was higher in the mid-wall (87%) and the subendocardium (78%) relative to the subepicardium (30%) across all canine ischemic episodes. In addition, the distributed pattern of ischemia (87%) was consistently observed regardless of the type or severity of acute ischemia. Finally, the relative frequency of occurrence of acute ischemia in the three defined regions was not significantly altered by repeated ischemia (Supplementary Data).

Figure 7 contains a summary of ischemia distribution resulting from studies across all 10 swine animals. The relative frequency of occurrence of acute ischemia was higher in the mid-wall (97%) and the subendocardium (94%) relative to the subepicardium (22%) across all swine ischemic episodes. In addition, the distributed pattern of ischemia (94%) was predominantly observed regardless of the type or severity of acute ischemia and comparable to that seen in canine studies. The effect of repeated episodes on the spatial distribution of acute ischemia was noted from the first to the second episode, but less so from the second to the third episode. Overall, the relative frequency of occurrence of acute ischemia in the three defined regions was not significantly altered by repeated ischemia and comparable to that seen in canine studies (Supplementary Data).

4 Discussion

The aim of this study was to evaluate the conventionally held assumptions about nontransmural ischemia using intramural electrodes to measure three-dimensional potential distributions in the ventricles of animals exposed to acute ischemia. To that end, we conducted a series of in situ experiments on canine and swine subjects and profiled the resulting intramural and epicardial potentials. We captured the spatial distribution of the electrocardiographic response acute myocardial ischemia under staged conditions of both supply and demand forms of the condition in both dogs and pigs. The two major findings from this study were a) acute ischemia originated not only in the subendocardium but throughout the ventricular wall, *i.e.,* in the subendocardium, midmyocardium, or the subepicardium, and b) The frequency of occurrence of acute ischemia was higher in the subendocardium and the mid-wall relative to the subepicardium. The most important conclusion from this study is that the electrical response of the heart to acute ischemic stress is not localized to the subendocardium, thus calling into doubt a major tenet of electrocardiography and the conventional explanation for primary ST segment depression.

Our choice of animal species follows the example of many past studies of ischemia and cardiac electrophysiology. Neither species is a perfect match to humans and so has strengths and weaknesses as an experimental model. Dogs have a conduction system more similar to that of humans [19], while it is the swine coronary vascular system that is more similar to that of humans [19]. The collateral circulation is more extensive in dogs compared to pigs, whereas the human collateral network falls somewhere between those two species [19]. Hence it is all the more meaningful that the results were consistent across both animal models, suggesting a fundamental mechanistic truth.

The study protocol was designed to simulate exercise testing or the very initial phase of a coronary spasm or myocardial infarct and thus focused on the most acute phase of ischemia. We designed the duration of ischemic episodes (2–10 minutes) to be within what is considered the reversible range [20], *i.e.,* a level of insult from which the heart would recover fully in a short time. To allow sufficient recovery between ischemic episodes, we followed each ischemic episode by 25–30 minutes of recovery. Jennings *et al.* have shown that such a recovery period is enough to restore normal ATP production and achieve reversal of changes in cellular ultrastructure [20]. The use of plunge needle electrodes to record intramural potentials resulted in some tissue trauma, which resolved quickly with little myocardial scarring or LV dysfunction [21].

We were able to induce acute ischemia when the perfusion deficit reached at least 50%, which is in agreement with other studies [22], [23]. In addition, we did not observe any meaningful shifts in the epicardial ST potentials during the onset of acute ischemia which is also in agreement with previous studies [24]. Moreover, epicardial ST segment elevation was observed only when acute ischemia reached transmural status. Interestingly, under the conditions of demand ischemia at rapid heart rates, we observed sharp epicardial ST segment depression overlapping the underlying non-transmural ischemia but spanning a much wider area and may be associated with increasing voltage gradients across the ischemic boundary [25]. Thus, the epicardial ST potentials were limited in their ability to localize the underlying non-transmural ischemia.

Our data demonstrated the acute ischemia arises throughout the myocardial wall. In Fig. 2, a canine complete occlusion study, acute ischemia arose in the subendocardium, mid-wall and the subepicardium. In Fig. 3, a canine supply ischemia study, acute ischemia originated in the subendocardium and the mid-wall region. In Fig. 4, a canine demand ischemia study, acute ischemia originated in the subendocardium. However, with increased stress, additional ST elevated regions were observed arising throughout the ventricular wall. In Fig. 5, a swine supply ischemia study, acute ischemia also originated in the mid-wall region. Thus, results from our study showed that acute ischemia is not always localized in the subendocardium and can arise throughout the myocardium.

Our data also demonstrated that the relative frequency of occurrence of acute ischemia was higher in the subendocardium and the mid-wall in comparison with the subepicardial region. The statistical summaries in Fig. 6 and Fig. 7 showed that the relative frequency of occurrence of acute ischemia was higher in the mid-wall (87% for canines, 97% for swines) and the subendocardium (78% for canines and 94% for swines) relative to the

subepicardium (30% for canines and 22% for swines). In addition, acute ischemia was seen arising throughout the myocardium (distributed pattern) in 87% of the canine and 94% of the swine episodes. Alternately, acute ischemia was seen always originating only in subendocardium (subendocardial pattern) in 13% of the canine episodes and 6% of the swine episodes. The frequency of occurrence across the three defined regions (Endo, Mid, Epi) stayed relatively consistent independent of the type and severity of ischemia. Studies [26] have suggested that repeated ischemia induces altered electrical response to subsequent ischemic episodes and is associated with attenuated metabolic response and increased conduction delay. The repeated ischemic episodes did not significantly alter the relative frequencies of occurrence between the three defined regions (Supplementary Data).

There is some evidence in the literature to support the possibility that ischemia would occur first in subendocardial zones. For example, some studies speculate that the subendocardium is the region most vulnerable to ischemia due to transmural gradients in regional blood flow [27], and others suggest the existence of intramyocardial pressure gradients [28] and greater metabolic stress [29]. Our results, however, do not support the resulting hypothesized consequences, none of which have actually been supported by high resolution measurements of three-dimensional parameters such as our studies describe.

Ours is not the only study to suggest heterogeneity of the ischemic response within the endocardium [30], [31], [32], [33], [34]. Steenbergen *et al.* [30] used NADH fluorescence photography in their rat model studies to show that ischemia produced by gradual reduction in coronary flow resulted in heterogeneous areas of anoxic tissue and attributed this response to intrinsic properties of arterioles. Gilmour *et al.* [31] studied the transmembrane potentials in a canine ischemia model to suggest that epicardial and papillary muscle excitability is more easily depressed during ischemia compared to endocardium, which is more responsive due to contact with the Purkinje fibers that provide continued electrical stimulation. Wilensky *et al.* [32] investigated transmembrane potentials in a rabbit model and suggested that during the first 10 minutes of ischemia, an endocardium rim layer, 60 cells deep (approximately 600 μ), remains unaffected by ischemia and may be attributed to multiple factors including diffusion of oxygen and nutrients from the cavity, blood transport via luminal vessels towards the subendocardial tissue, electrical coupling with Purkinje fibers, and greater resistance of subendocardial cells to effects of hypoxia, elevated extracellular potassium, and acidosis. Austin *et al.* [33], based on measurements of canine regional blood flow, suggested spatial heterogeneity of myocardial perfusion within the endocardium, resulting in islands of viable subendocardial tissue due to differences in local metabolic demand secondary to differences in regional function. Leshnower *et al.* [34], in an irreversible ischemia study on sheep, found that the midmyocardium was most vulnerable to ischemia and the subendocardium was most resistant. Franzen *et al.* [35] demonstrated substantial spatial heterogeneity in local blood flow and metabolite content in their canine studies and suggested that at microvascular level both blood flow and metabolism behave heterogeneously from their neighboring units. In addition, previous acute ischemia studies on canines [36] and swines [37] have suggested that the spatial heterogeneity in local extracellular K^+ concentrations may be associated with differences in membrane sensitivity to acute ischemia, different rates of ATP depletion, and intersite diffusion of K^+ ions. Even if there remains uncertainly as to specific mechanisms, there is emerging agreement from our

and other findings calling into doubt the prevailing notion that the onset of ischemia is limited to the subendocardium.

The clinical accuracy of the electrocardiogram (ECG) to detect and localize myocardial ischemia remains less than satisfactory [1], and our findings suggest possible mechanisms for this poor performance. ECG leads that show ST segment elevation provide a means of localizing transmural ischemia from the body surface and are a well-known clinical marker of infarction [38]. This was also evident in our study with epicardial ST elevation observed when acute ischemia reached transmural status. However, the ability of ST segment depression to locate ischemia is considerably less specific [10]. Acute ischemia studies with animal models have shown that even on the cardiac surface (epicardium), ST segment changes have poor sensitivity [24]. Our data also demonstrated that nontransmural ischemia is often undetected on the epicardial surface, especially using the ST segment as a marker. This behavior was consistently seen across both canine and swine species and could be associated with one or more of the following: a) signal attenuation due to distance from the epicardium, b) masking effect from other nearby ischemia sources, and c) electrical anisotropy, with higher resistance to current flow towards the epicardium. It is possible then that the superposition of these discrete ischemic sources may attenuate or neutralize resulting injury currents, limiting the ability of the epicardial electrograms to detect and localize nontransmural ischemia. Indeed, the consequences of this ambiguity on the body-surface ECG remains a topic of ongoing research but are likely to be even less predictive than the more proximal and spatially resolved epicardial potentials. Results from our previous study [39] have shown that under the conditions of very acute ischemia, epicardial T-waves have higher sensitivity to mild degrees of acute ischemia than epicardial ST segment potentials. Moreover, epicardial QRS potentials showed even less sensitivity to mild ischemia than the ST segment and thus had limited ability to localized the spatial extent or degree of myocardial ischemia. This suggests that a combination of epicardial ST segment and T-wave markers could provide a more reliable index of acute ischemia than either in isolation.

5 Limitations

Our study has several limitations. First, we did not measure myocardial collateral blood flow which would have provided information on regional primary and collateral blood flow to compare with the electrical recordings. Instead, the findings of this study depend on the assumption that local shifts in extracellular ST segment potentials can be detected with sufficient spatial resolution and that they reflect nearby ischemia. While an indirect marker of what is fundamentally a perfusion deficit, intramural extracellular ST segment potentials have been shown to be a sensitive marker for ischemia [24] and correlate well with regional blood flow [40] and local gas tension measurements [41].

Second, the insertion of plunge needles causes tissue trauma. However, the plunge needle electrodes we used were finer than previously available, creating significantly less tissue injury, and therefore more sensitive measurements than possible in previous studies. In addition, we benefited from the most detailed and comprehensive electrical measurements reported to date: a 247-electrode sock array to record epicardial potentials and up to 250

needle electrodes to measure intramural potentials, thus providing a high degree of three-dimensional spatial resolution. Moreover, the spatial resolution of our intramural recordings was 1.5 mm along each needle and 10 mm between neighboring needles, thus enabling a precise enough identification of intramural ischemia at the several millimeter scale we measured it.

Third, the LAD occlusion procedure to identify the perfusion bed could have preconditioned the myocardium affecting the the spatial distribution of acute ischemia during the subsequent interventions. However, the acute phase of preconditioning is believed to last up to 120 minutes [42], and in our studies, the recovery period after the initial occlusion procedure was typically 90 minutes or more to account for plunge needle insertion procedure and the subsequent stabilization period. This may have mitigated the preconditioning effect on the myocardium.

6 Conclusion

In summary, our results suggest a complex electrocardiographic response to acute ischemia characterized by heterogeneous distribution of ST segment elevated regions across the myocardial wall. Understanding the spatial and temporal nature of these underlying bioelectric sources may provide future insights into ways to localize ischemia from the cardiac surface and may impact how we interpret potentials measured on the body surface. A possible approach we have also begun to evaluate successfully is to identify other electrical markers (T-wave, QRS complex, *etc.,*) in combination with ST segment that could improve the ability to detect and localize the extent of myocardial injury [39]. At a minimum, the spatial heterogeneity of the ischemic response that we have documented suggests a need to refine the current electrocardiographic model of ischemia.

Supplementary Material

Refer to Web version on PubMed Central for supplementary material.

Acknowledgements

Support for this research comes from the NIH NIGMS Center for Integrative Biomedical Computing (www.sci.utah.edu/cibc), NIH NIGMS Grant No. P41GM103545, the Nora Eccles Treadwell Foundation, and the Nora Eccles Treadwell Foundation for Cardiovascular Research. We also wish to thank Ms. Jayne Davis and Ala Booth, Dr. Phil Ershler, and Mr. Bruce Steadman for their valuable assistance in performing the experiments described here.

References

1. Gorgels A. ST elevation and non-ST elevation acute coronary syndromes: Should the guidelines be changed? Journal of Electrocardiology. 2013; 46(4):318–323. [PubMed: 23688768]
2. O'Rourke, R.; O'Gara, P. Hurst's the Heart - Diagnosis and Management of Patients with CID. McGraw-Hill; New York: 2010. 1em plus 0.5em minus 0.4em
3. Reimer, K.; Jennings, R. Myocardial ischemia, hypoxia and mi. In: Fozzard, H., et al., editors. The Heart and Cardiovascular System. Raven Press; New York: 1986. p. 1133-2101.1em plus 0.5em minus 0.4em

4. Kleber A, Janse M, van Capelle F, Durrer D. Mechanism and time course of ST and TQ segment changes during acute regional myocardial ischemia in the pig heart determined by extracellular and intracellular recordings. Circulation Research. 1978; 42:603–613. [PubMed: 639183]
5. Kubota I, Yamaki M, Shibata T, Ikeno E, Hosoya Y, Tomoike H. Role of ATP-sensitive channel on ECG ST segment elevation during a bout of myocardial ischemia. Circulation. 1993; 88:1845–1851. [PubMed: 8403330]
6. Savage R, Wagner G, Ideker R, Podolsky S, Hackel D. Correlation of postmortem anatomic findings with electrocardiographic changes in patients with myocardial infarction. Circulation. 1977; 5:279–285. [PubMed: 832343]
7. Kléber A. Extracellular potassium accumulation in acute myocardial ischemia. Journal of Molecular and Cellular Cardiology. 1984; 16:389–394. [PubMed: 6737481]
8. Janse M, Cinca J, Morena H, Fiolet J, Kleber A, de Vries G, Becker A, Durrer D. The border zone in myocardial ischemia. An electrophysiological, metabolic and histochemical correlation in the pig heart. Circulation Research. 1979; 44:576–588. [PubMed: 428053]
9. Rogers J, Melnick S, Huang J. Fiberglass needle electrodes for transmural cardiac mapping. IEEE Transactions in Biomedical Engineering. 2002; 49:111–118.
10. Guyton R, McClenathan J, Newman G. Significance of subendocardial ST segment elevation caused by coronary stenosis in the dog. American Journal of Cardiology. 1977; 40:373–380. [PubMed: 900035]
11. Shome, S.; Stinstra, J.; Hopenfeld, B.; Punske, B.; MacLeod, R. Proceedings of the IEEE Engineering in Medicine and Biology Society 26th Annual International Conference, IEEE EMBS. IEEE Press; 2004. A study of the dynamics of cardiac ischemia using experimental and modeling approaches. 1em plus 0.5em minus 0.4em
12. Mirvis D, Gordey R. Electrocardiographic effects of myocardial ischemia induced by atrial pacing in dogs with coronary stenosis. Repolarization changes with progressive left circumflex coronary artery narrowing. Journal of American College of Cardiology. 1983; 4:1090–1098.
13. Arisi G, Macchi E, Corradi C, Lux R. Epicardial excitation during ventricular pacing. Relative independence of breakthrough sites from excitation sequence in canine right ventricle. Circulation Research. 1992; 71:840–849. [PubMed: 1381295]
14. Ershler P, Steadman K, Moore K, Lux R. Systems for measuring and tracking electrophysiological distributions: Current tools for clinical and experimental cardiac mapping. IEEE Transactions in Biomedical Engineering. 1998; 26:56–61.
15. Cinca J, Janse M, Morena H, Candell J, Valle V, Durrer D. Mechanism and time course of the early electrical changes during acute coronary artery occlusion. Chest. 1980; 77:188–204. [PubMed: 7353412]
16. Institute, S. map3d: Interactive scientific visualization tool for bioengineering data. Scientific Computing and Imaging Institute (SCI). download from: http://www.scirun.org, 2015
17. Institute S. Seg3D: Volume segmentation and processing tool. Scientific Computing and Imaging Institute (SCI). 2015 download from: http://www.scirun.org.
18. Institute, S. SCIRun: A scientific computing problem solving environment. Scientific Computing and Imaging Institute (SCI). 2015. download from: http://www.scirun.org
19. Verdouw P, Wolffebuttel B, Giessen J. Domestic pigs in the study of myocardial ischemia. European Heart Journal. 1983; 4:61–67. [PubMed: 6352271]
20. Jennings R, Ganote C, Reimer K. Ischemic tissue injury. American Journal of Pathology. 1975; 81:179–198. [PubMed: 1180331]
21. Kovoor P, Campbell C, Wallace E, Byth K, Dewsnap B, Eipper V, Uther J, Ross D. Effects of simultaneous insertion of 66 plunge needle electrodes on myocardial activation, function, and structure. PACE. 2003; 26:1979–1985. [PubMed: 14516338]
22. Mori H, Ogawa S, Hayashi J, Osuzu F, Hattori S, Takahashi M, Hara K, Tanabe Y, Nakamura Y. Electrophysiologic and myocardial metabolic changes in the acute phase of partial coronary occlusion. American Heart Journal. 1983; 106:624–630. [PubMed: 6613806]
23. Kingaby R, Lab M, Cole A, Palmer T. Relation between monophasic APD, ST elevation, and regional blood flow after coronary occlusion in pig. Cardiovascular Research. 1986; 20:740–751. [PubMed: 3791340]

24. Watanabe I, Johnson T, Buchanan J, Engle C, Gettes L. Effect of graded coronary flow reduction on ionic, electrical, and mechanical indexes of ischemia in the pig. Circulation. 1987; 76:1127–1134. [PubMed: 3664997]
25. Kligfield P. Principles of simple heart rate adjustment of ST segment depression during exercise electrocardiography. Cardiology Journal. 2008; 15:194–200. [PubMed: 18651407]
26. Saito T, Miura H, Kimura Y, Watanabe H, Nakagomi A, Tamura Y, Hasegawa H, Kibira S, Miura M. Reduction of ST elevation in repeated coronary occlusion model depends on both altered metabolic response and conduction property. International Journal of Cardiology. 2003; 92:219–227. [PubMed: 14659856]
27. Li D, Li C, Yong A, Kilpatrick D. Source of electrocardiographic ST changes in subendocardial ischemia. Circulation Research. 1998; 82:957–970. [PubMed: 9598593]
28. Sabbah H, Stein P. Effect of acute regional ischemia on pressure in the subepicardium and subendocardium. American Journal of Physiology. 1982; 242:H240–H244. [PubMed: 7065158]
29. Fujiwara H, Ashraf M, Sato S, Millard R. Transmural cellular damage and blood flow distribution in early ischemia in pig hearts. Circulation Research. 1982; 51:683–693. [PubMed: 6754127]
30. Steenbergen C, Deleeuw C, Barlow C, Chance B, Williamson J. Heterogeneity of the hypoxic state in perfused rat heart. Circulation Research. 1977; 41:606–615. [PubMed: 908108]
31. Gilmour R, Zipes D. Different electrophysiological responses of canine endocardium and epicardium to combined hyperkalemia, hypoxia and acidosis. Circulation Research. 1980; 46:814–825. [PubMed: 7379247]
32. Wilensky R, Tranum-Jensen J, Coronel R, Wilde A, Fiolet J, Janse M. The subendocardial border zone during acute ischemia of the rabbit heart: An electrophysiologic, metabolic and morphologic correlative study. Circulation. 1986; 74:1137–1146. [PubMed: 3769171]
33. Austin R, Aldea G, Coggins D, Flynn A, Hoffman J. Profound spatial heterogeneity of coronary reserve - Discordance between patterns of resting and maximal myocardial blood flow. Circulation Research. 1990; 67:319–331. [PubMed: 2376074]
34. Leshnower B, Sakamoto H, Hamamoto H, Zeeshan A, Gorman J, Gorman R. Progression of myocardial injury during coronary occlusion in the collateral-deficient heart: A non wavefront phenomenon. American Journal of Physiology. 2007; 293:1799–1804.
35. Franzen D, Conway R, Zhang H, Sonnenblick E, Eng C. Spatial heterogeneity of local blood flow and metabolite content in dog hearts. American Journal of Physiology. 1988; 254:344–353.
36. Hariman R, Louie E, Krahmer R, Bremner S, Euler D, Hwang M, Ferguson J, Loeb H. Regional changes in blood flow, extracellular potassium and conduction during myocardial ischemia and reperfusion. Journal of Amercian College of Cardiology. 1993; 21:798–808.
37. Johnson T, Engle C, Boyd L, Koch G, Gwinn M, Gettes L. Effect of exercise intensity and duration on regional function during and after exercise-induced ischemia. Circulation. 1991; 83:622–634. [PubMed: 1991380]
38. Wagner, G. Marriott's Practical Electrocardiography. 11th ed.. Lippincott Williams & Wilkins; Philadelphia: 2008. 1em plus 0.5em minus 0.4em
39. Aras K, Burton B, Swenson D, MacLeod R. Sensitivity of epicardial electrical markers to acute ischemia detection. Journal of Electrocardiology. 2014; 47(6):836–841. [PubMed: 25242529]
40. Lekven J, Ilebekk A, Fonstelien E, Kil F. Relationship between ST segment elevation and local tissue flow during myocardial ischaemia in dogs. Cardiovascular Research. 1975; 9:627–633. [PubMed: 1201571]
41. Khuri S, Flaherty J, O'Riordan J, Pitt B, Brawley R, Donahoo J, Gott V. Changes in intramyocardial ST segment voltage and gas tensions with regional myocardial ischemia in the dog. Circulation Research. 1975; 37:455–463. [PubMed: 1182937]
42. Yellon D, Downey J. Preconditioning the myocardium: From cellular physiology to clinical cardiology. Physiology Reviews. 2003; 83:1113–1151.

Review Highlights

- We conducted acute ischemia studies in open-chest canines and swines and recorded intramyocardial and epicardial potentials.
- Acute ischemia was characterized by pockets of ST-segment elevated regions variously distributed in subepicardial, mid-wall, and subendocardial regions.
- Spatial distribution of acute ischemia is a complex phenomenon spread throughout the myocardial wall and is not limited to the subendocardium.

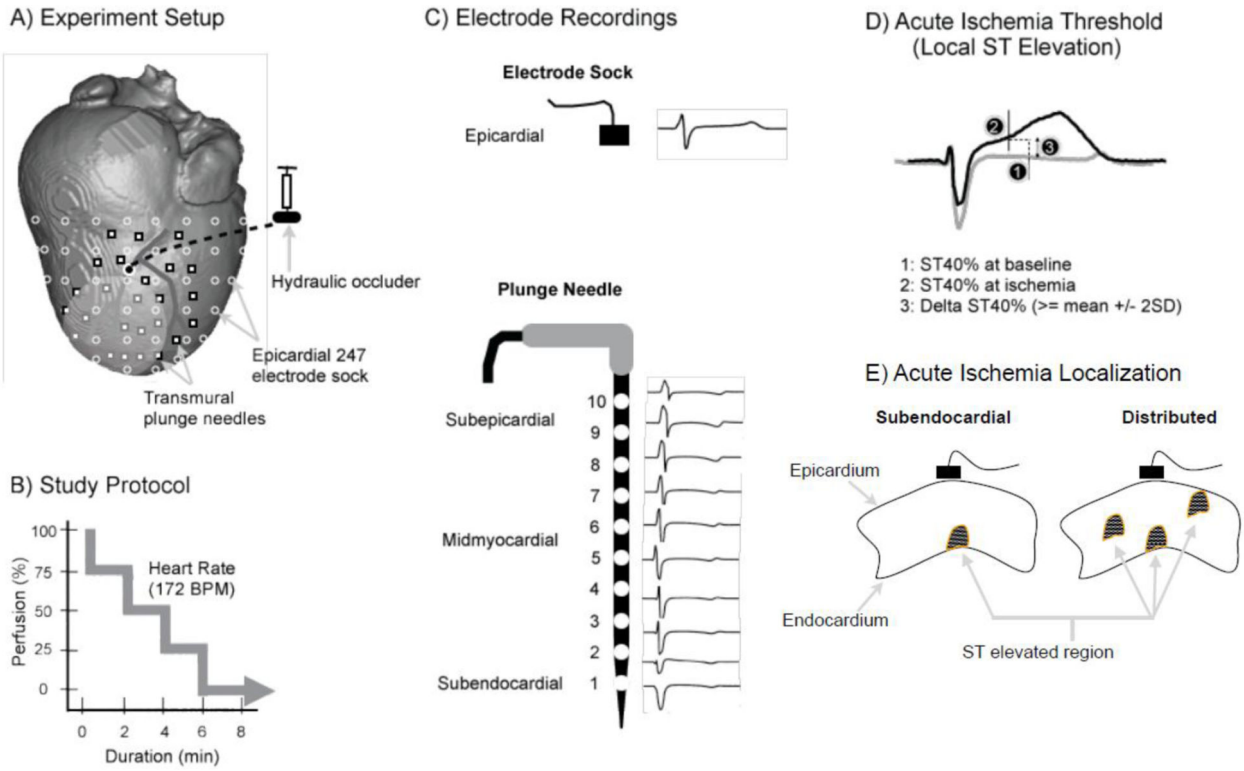

Figure 1.

Experiment setup: (a) Experiment setup, (b) sample study protocol, (c) sample epicardial and intramural electrograms, (d) ischemia threshold based on localized ST40% potential. (e) schematic of subendocardial and distributed patterns of ischemia localization

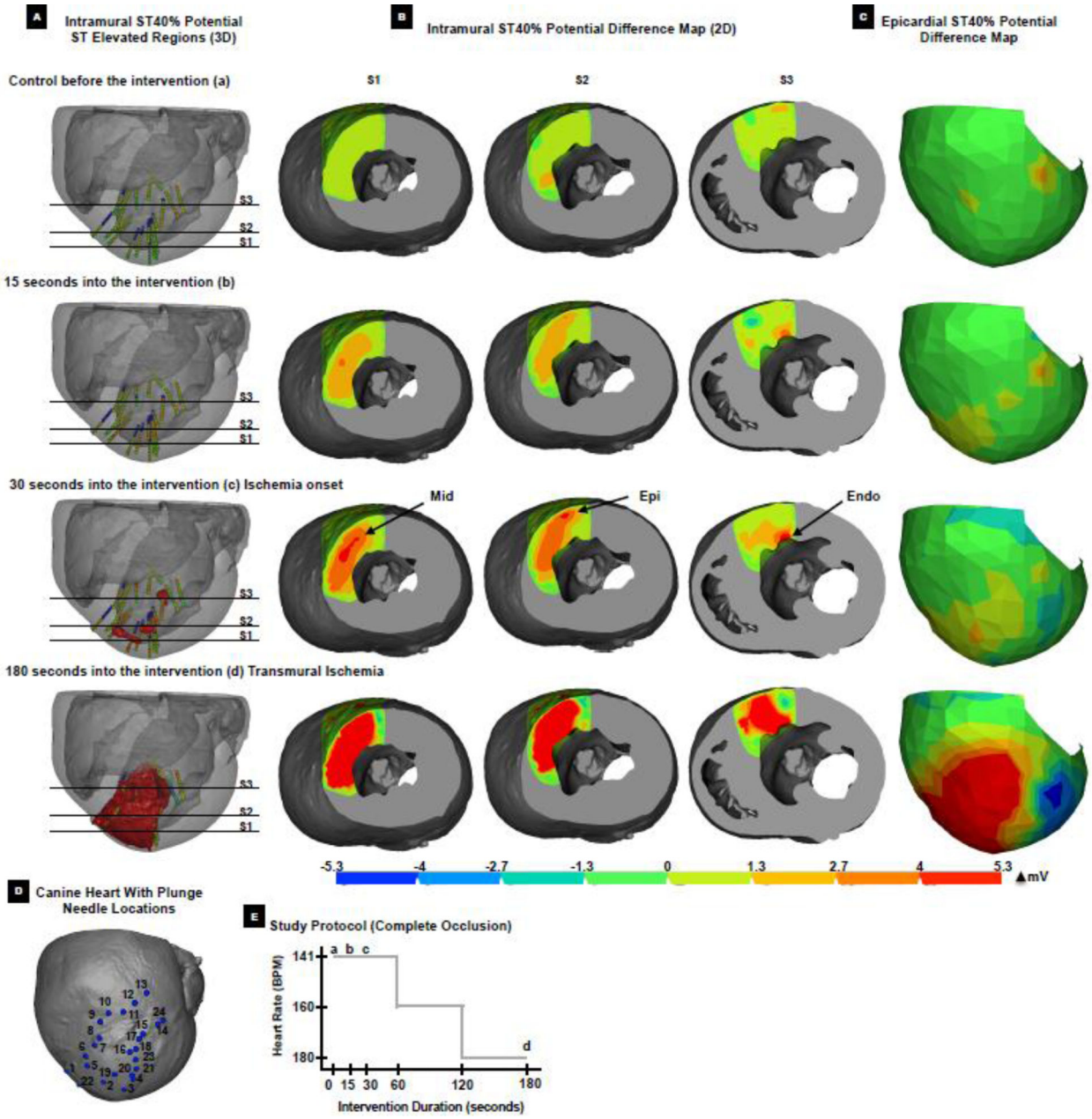

Figure 2.

Canine ventricular response to complete occlusion demonstrating that acute ischemia arises throughout the myocardium including the subendocardium, mid-wall and sub-epicardium. A) Intramural ST40% potential difference map (ischemic volume). B) Intramural ST40% potential difference map (surface distribution) corresponding to the three axial slices (S1, S2, S3) in panel A. C) Epicardial ST40% potential difference map. D) Canine heart with location of the plunge needles. E) Complete occlusion study protocol. The rows correspond to the time points during the ischemic episode and marked in panel E: a) control, b) 15 seconds into the intervention, c) 30 seconds into the intervention, and d) 180 seconds into the intervention.

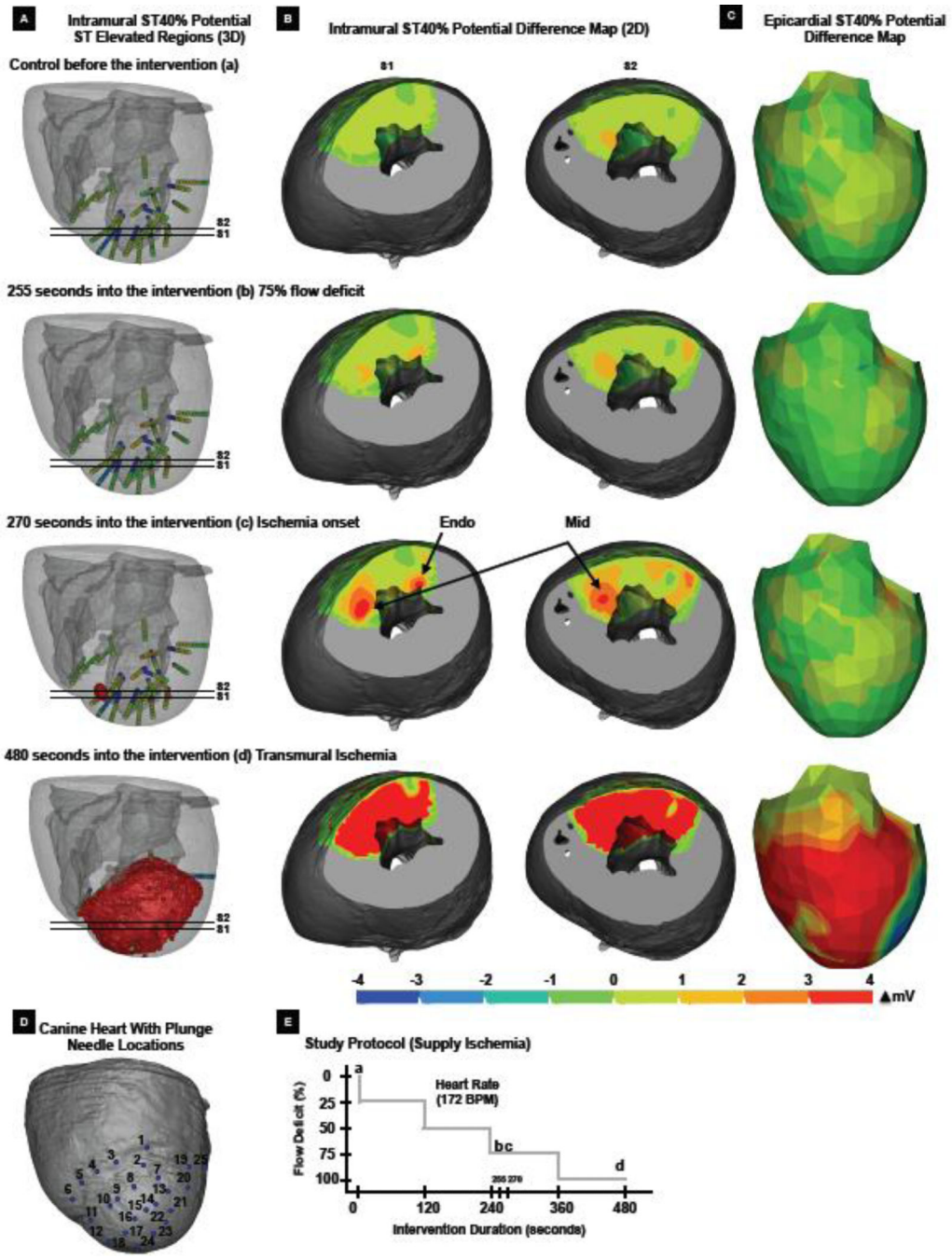

Figure 3.

Canine ventricular response to supply ischemia @ 172 BPM showing that acute ischemia arises throughout the myocardium and in this instance the subendocardium and the mid-wall region. A) Intramural ST40% potential difference map (ischemic volume). B) Intramural ST40% potential difference map (surface distribution), corresponding to the two axial slices (S1, S2) in panel A. C) Epicardial ST40% potential difference map. D) Canine heart with location of the plunge needles. E) Supply ischemia study protocol. The rows correspond to the time points during the ischemic episode and marked in panel E: a) control, b) 255

seconds into the intervention, c) 270 seconds into the intervention, and d) 480 seconds into the intervention.

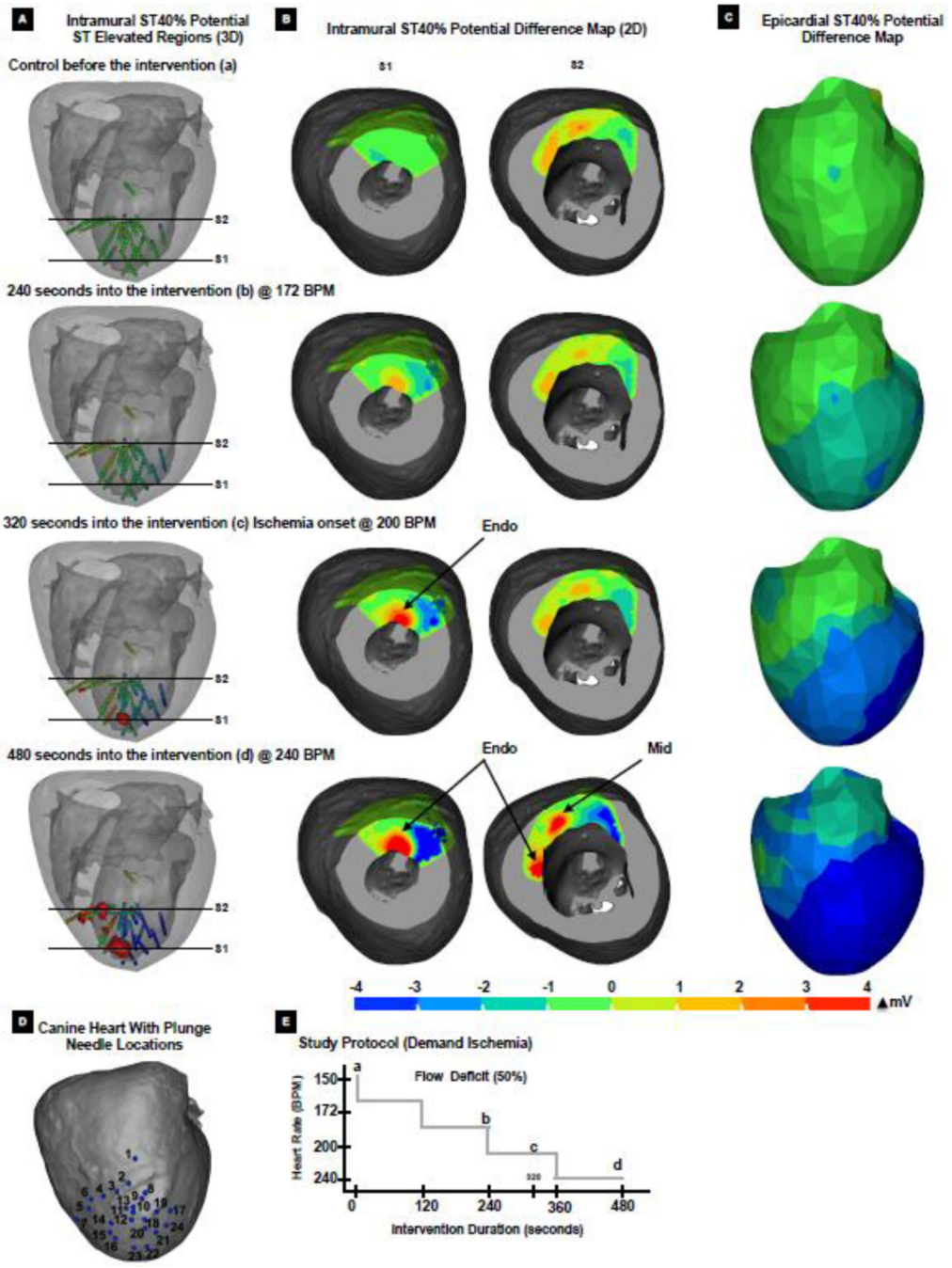

Figure 4.

Canine ventricular response to demand ischemia @ 50% perfusion deficit showing that acute ischemia arises throughout the myocardium and in this instance the subendocardium and the mid-wall region. A) Intramural ST40% potential difference map (ischemic volume). B) Intramural ST40% potential difference map (surface distribution), corresponding to the two axial slices (S1, S2) in panel A. C) Epicardial ST40% potential difference map. D) Canine heart with location of the plunge needles. E) Demand ischemia study protocol. The rows correspond to the time points during the ischemic episode and marked in panel E: a) control,

b) 240 seconds into the intervention, c) 320 seconds into the intervention, and d) 480 seconds into the intervention.

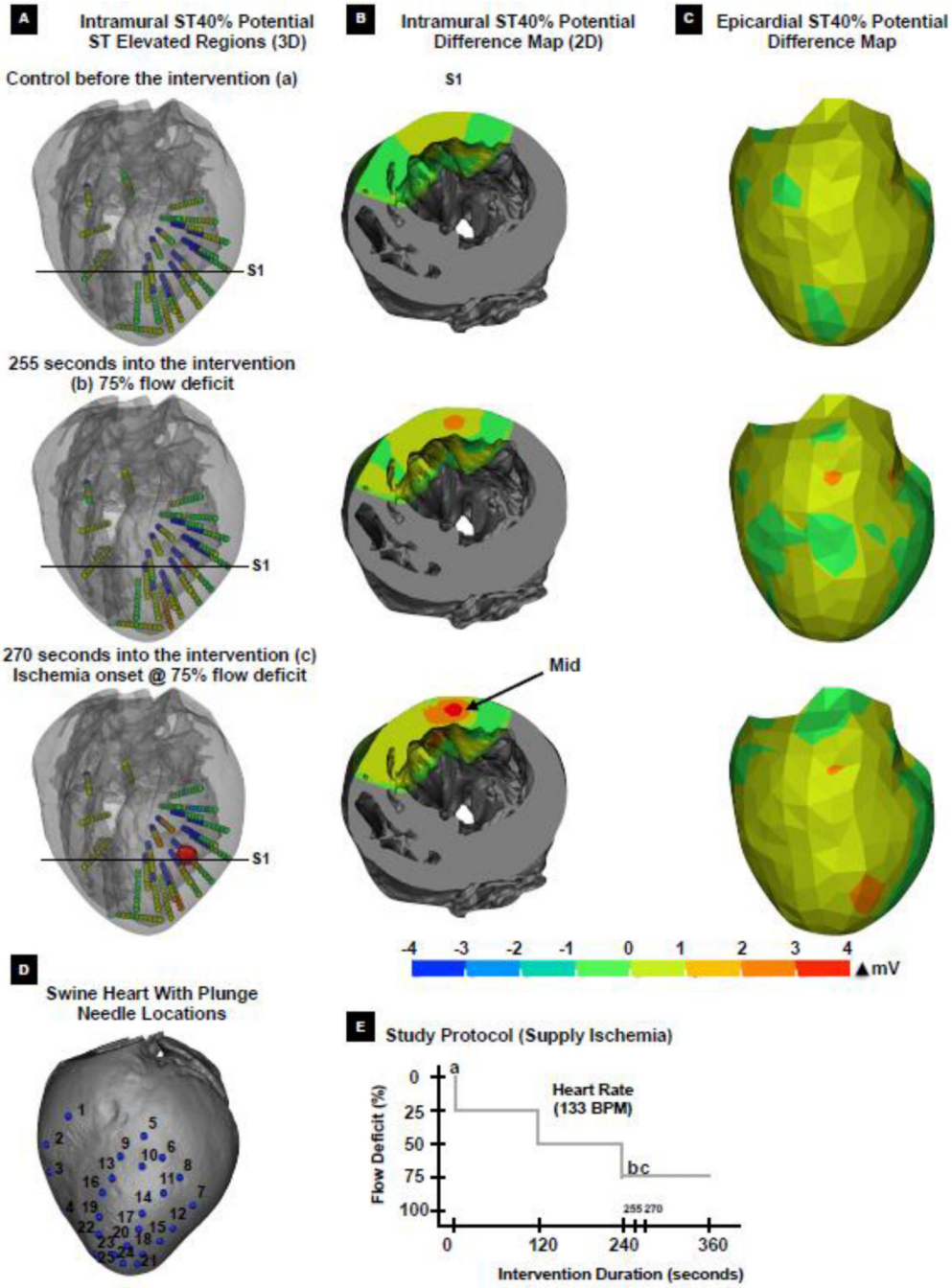

Figure 5.

Swine ventricular response to supply ischemia @ 133 BPM demonstrating that acute ischemia is not always localized in the subendocardium and in this instance arises in the mid-wall region. A) Intramural ST40% potential difference map (ischemic volume). B) Intramural ST40% potential difference map (surface distribution), corresponding to the axial slice (S1) in panel A. C) Epicardial ST40% potential difference map. D) Swine heart with location of the plunge needles. E) Supply ischemia study protocol. The rows correspond to

the time points during the ischemic episode and marked in panel E: a) control, b) 255 seconds into the intervention, and c) 270 seconds into the intervention.

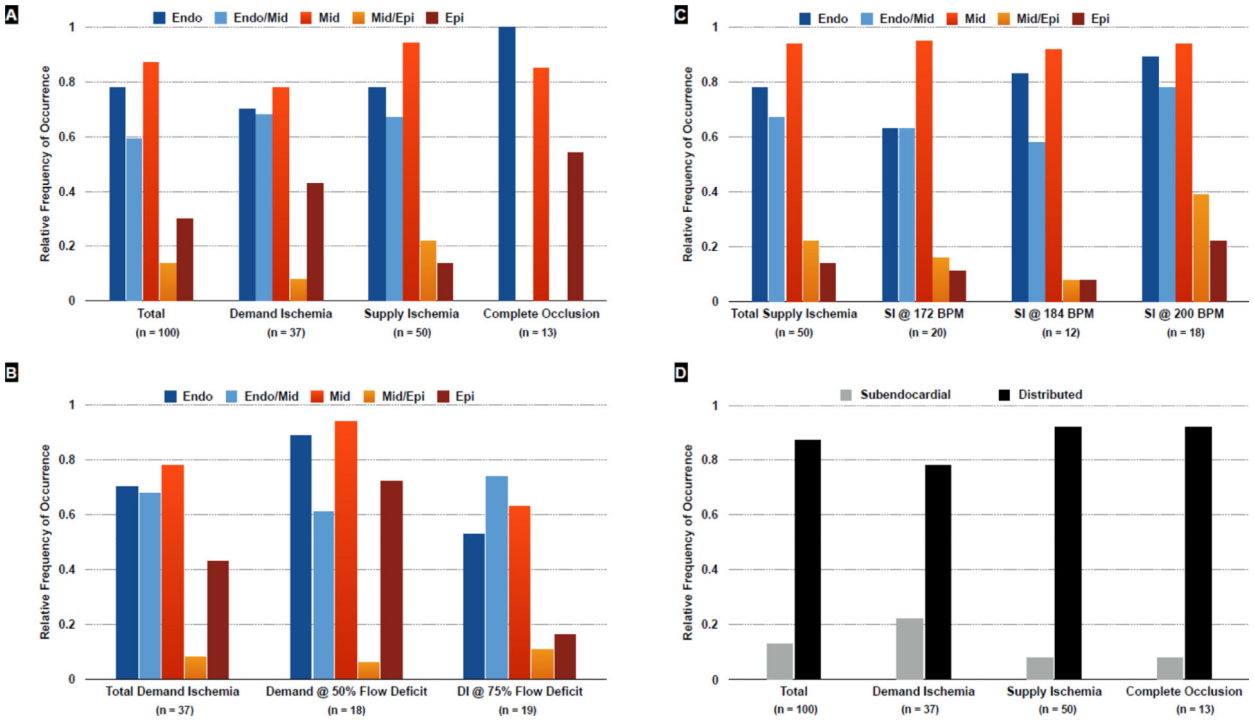

Figure 6.

Statistical summary of ischemia distribution across all canine studies demonstrating higher frequency of spatial distribution in the subendocardium and mid-wall regions relative to the subepicardial region. In addition, the distributed pattern of ischemia is the dominant pattern regardless of the type and severity of ischemia. The histograms quantify the relative frequency of occurrence of acute ischemia in each of the three defined regions as well as the two overlapping regions for A) cumulative, B) demand ischemia, and C) supply ischemia episodes. D) The histograms of relative frequency of occurrence of acute ischemia grouped by subendocardial or distributed pattern of localization (cumulative). The figures capture a total of 100 episodes of ischemia in canines.

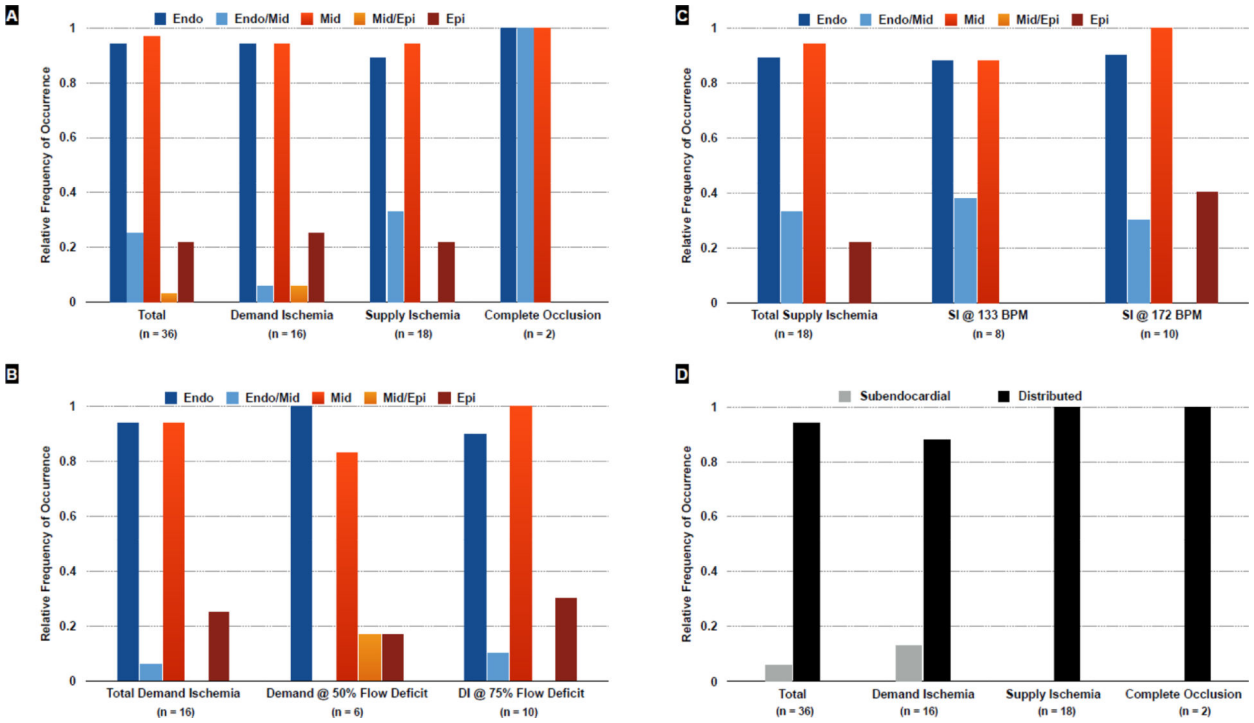

Figure 7.

Statistical summary of ischemia distribution across all swine studies demonstrating higher frequency of spatial distribution in the subendocardium and mid-wall regions relative to the subepicardial region. In addition, the distributed pattern of ischemia is the dominant pattern regardless of the type and severity of ischemia. The histograms quantify the relative frequency of occurrence of acute ischemia in each of the three defined regions as well as the two overlapping regions for A) cumulative, B) demand ischemia, and C) supply ischemia episodes. D) The histograms of relative frequency of occurrence of acute ischemia grouped by subendocardial or distributed pattern of localization (cumulative). The figures capture a total of 36 episodes of ischemia in swines.